Pozzo, L.Y.de; da Conceicao, T.F.; Spinelli, A.; Scharnagl, N.; Nunes Pires, A.T.:

The influence of the crosslinking degree on the corrosion protection properties of chitosan coatings in simulated body fluid.

In: Progress in Organic Coatings. Vol. 137 (2019) 105328.
First published online by Elsevier: 21.09.2019

https://dx.doi.org/10.1016/j.porgcoat.2019.105328

The influence of the crosslinking degree on the corrosion protection properties of chitosan coatings in simulated body fluid

Ludmila de Y. Pozzo[a], Thiago F. da Conceição [b*], Almir Spinelli [b], Nico Scharnagl [c], Alfredo T. Nunes Pires [b]

[a] Department of Materials Engineering, Federal University of Santa Catarina, 88040-900 Florianópolis, SC, Brazil

[b] Department of Chemistry, Federal University of Santa Catarina, 88040-970 Florianópolis, SC, Brazil

[c] Helmholtz-Zentrum Geesthacht GmbH, Institute of Materials Research, Magnesium Innovations Centre - MagIC, Max-Planck-Str. 1, D-21502 Geesthacht, Germany

*e-mail: thiago.conceicao@ufsc.br

Abstract

This paper describes the protection of magnesium AZ31 alloy sheets in a simulated body fluid (SBF) medium provided by chitosan coatings. It demonstrates, by means of potentiodynamic polarization curves and electrochemical impedance spectroscopy, that chitosan coatings with a crosslinking degree of up to 42% are efficient in protecting the alloy in SBF, with a performance superior to similar coatings reported in the literature. With higher crosslinking degrees the coating becomes brittle and susceptible to cracks, decreasing its protective properties. The hydrogen evolution rate observed for the best coating complies with the acceptance level and further demonstrates its potential to control the degradation of magnesium alloy implants.

Keywords: coating materials, corrosion, electrochemical impedance spectroscopy, SEM

1. Introduction

The development of environment-friendly coatings and inhibitors to control the corrosion of metallic materials is of great relevance in modern society. Costs associated with corrosion have a considerable impact on the economy of developed countries, and traditional corrosion inhibition methods are subject to legal restrictions [1]. Thus, the development of new effective anti-corrosion methods, based on natural or biodegradable chemicals, is receiving increasing interest. Recent reports in the literature verify the potential of natural chemicals, such as phytic acid [2, 3], vanillic acid [4] and stearic acid [5], and of natural polysaccharides, such as gum arabic [6], konjac-glucomannan [7], alginate [8], pectins [9, 10] and chitosan [11, 12] to act as corrosion inhibitors and as protective coatings for different metals. Chitosan is notably the most studied and promising of the above-mentioned polysaccharides.

Chitosan coatings have been applied to stainless steels [13-15], titanium alloys [16, 17], aluminum alloys [18] and magnesium alloys [19] among other materials. The influence of different parameters on the protective properties of these coatings is described in detail in the literature. Heise et al. [20], for instance, reported the positive effect of the pre-treatment of the magnesium alloy WE43 with Dulbecco's modified Eagle's medium on the protective properties of chitosan/bioactive-glass coatings prepared by electrophoretic deposition. In a study by Bai et al. [21], it was shown that the performance of chitosan coatings on a Mg-Zn-Ca magnesium alloy is considerably improved by a previous micro-arc oxidation process. Chitosan has also been chemically functionalized in order to increase its hydrophobic character [22]. In this cited study, chitosan was functionalized with poly(ethylene-*alt*-maleic anhydride) and poly(maleic anhydride-*alt*-1-octadecene) to form a protective coating with a hydrophobic surface on the aluminum alloy AA2024.

The literature also reports studies in which chitosan was combined with other polymers, such as cellulose acetate [13], collagen [23], alginate [24] and mussel adhesive proteins [25], to form multilayer coatings for the corrosion protection of different metals. Interestingly, the effect of crosslinking has not received much attention. Sugama & Cook [26] investigated the effect of chitosan crosslinking with poly(itaconic acid) on its protective properties as a coating on aluminum substrates Pozzo et al. [12] reported the protective properties of chitosan coatings crosslinked with

genipin on AZ31 magnesium alloys. It was showed that, for corrosion tests performed with 3.5 wt.% NaCl solutions, the level of protection provided by the coatings increases with the crosslinking degree.

Magnesium alloys are the lightest of the metallic materials that have been coated with chitosan and they present several interesting properties for automotive and biomedical applications. The strength-to-weight ratio of these alloys makes them suitable to replace steels and aluminum in vehicles, resulting in a considerable weight reduction and consequently reducing the fuel consumption [27]. Many different corrosion protection methods, from alloy design [28, 29] to the application of coatings [30-35], have been developed to improve the corrosion resistance of magnesium alloys and enhance their applicability.

From a biomedical point of view, magnesium and many of its alloys are very interesting materials, since they can be used for the fabrication of bioresorbable implants, in the form of screws for bone fixation and stents for vessel dilatation, due to their biodegradability and non-toxicity [36, 37]. Nevertheless, the temporary implant degradation must take place at a rate that allows the tissue recovery and avoids a high concentration of corrosion products in a given area, since this may cause inflammation [36]. Thus, it is necessary to cover the implants with biocompatible, bioabsorbable and biodegradable coatings.

The aim of this study was to investigate the influence of the crosslinking degree of chitosan coatings, crosslinked with genipin, on the corrosion protection of the magnesium alloy AZ31 in a simulated body fluid (SBF) medium. This alloy was selected due to the interesting results obtained in *in vivo* and *in vitro* tests on AZ31 implants [37-38]. The hypothesis under investigation is that the crosslinking of chitosan with genipin is an effective way to improve the anticorrosion properties of chitosan coatings in SBF. The effect of the different ions present in the SBF is discussed in detail, based on results obtained by potentiodynamic polarization and electrochemical impedance spectroscopy (EIS).

2. Materials and methods

2.1 Materials

The sheets of the AZ31 magnesium alloy used in this study have the dimensions of 5.0 x 2.0 x 0.2 cm and the following chemical composition in wt.%: Al 2.97; Zn 0.85; Mn 0.24; Si 0.02; Fe 0.03; Cu, Ca and Ni < 0.01; and Mg = Bal. Chitosan, (average molecular weight of 161,000 g mol^{-1} and degree of deacetylation of 75-85%), sodium hydroxide and acetic acid were obtained from Sigma Aldrich, whereas genipin (98% purity) was obtained from Challenge Bioproducts, Taiwan. All chemicals were used without further purification.

2.2 Methods

2.2.1 Preparation of coatings

The coatings were prepared as described in a previous publication of the authors [12]. In short, a previously ground (1200-grit paper) and NaOH treated sheet (2.0 mol L^{-1} at 90°C under mechanical stirring for 24 h) was dip coated with chitosan solutions (2.0 wt.%) in 0.5% of acetic acid in water, containing 0, 1, 3 or 6 mmol of genipin per mol of repeat unit. Then, the coatings were dried at room temperature for 24 h and under vacuum at 100 °C for 3 h. The final dry thickness of the coatings were in the order of 4-6 μm, as determined using a coating thickness gauge. The as-received, ground and NaOH treated samples were denoted as AZ31, AZ31Gr and AZ31T, respectively. The samples coated with neat chitosan and chitosan crosslinked with 1, 3 and 6 mmol of genipin were denoted as AZ31Q, AZ31G1, AZ31G3 and AZ31G6, respectively.

2.2.2 Electrochemical analysis

Electrochemical impedance spectroscopy (EIS) was performed using a three electrode cell (graphite rod as the auxiliary electrode, Ag/AgCl (saturated KCl) as the reference electrode and the sample as the working electrode) with the potentiostat PalmSens 3. After 30 min of open circuit potential (OCP) stabilization, a sinusoidal perturbation of 10 mV, in relation to OCP, was applied to the working electrode, in a frequency range from 100 kHz to 10 mHz. An area of approximately 1.0 cm^2 was exposed to a simulated body fluid (SBF) with the following composition in g L^{-1}: NaCl

8.00, KCl 0.40, $CaCl_2$ 0.14, $MgSO_4.7H_2O$ 0.20, Na_2HPO_4. $12H_2O$ 0.12, KH_2PO_4 0.06, $NaHCO_3$ 0.25 and d-glucose 1.0, at a pH of 7.4. Two measurements were performed for each sample. The impedance spectra were fitted using equivalent circuits (given in Fig. 3), in which pure capacitors were replaced by constant-phase elements (CPE). The software used for the fitting was EISSA1.

The potentiodynamic polarization experiments were performed for qualitative purposes using the same system and electrolyte described above. A scan rate of 0.1 mV s^{-1}, from -250 mV to 500 mV in relation to the OCP, was applied to the working electrode, after a period of 30 min for system stabilization. The current limit was set at 10 mA. Four measurements were performed for each sample.

2.2.3 Hydrogen evolution

The rate of hydrogen evolution was measured for selected samples using the traditional setup comprised of a beaker, a funnel and a burette, as described elsewhere [39]. The selected samples were mounted in an epoxy resin to control the exposure area (approximately 5 cm^2). The samples were exposed to 100 mL of SBF at room temperature, for 7 days, and the volume of gas evolved was measured each day. Three samples were measured for each treatment condition.

2.2. 4 Ninhydrin assay

To investigate whether the SBF would react with the coatings and change their crosslinking degree, free-standing films of neat chitosan (QT) and of chitosan crosslinked with 1 (QTG1), 3 (QTG3) and 6 (QTG6) mmol of genipin were prepared. The percentage of free amine (FA) in the films, before and after immersion in SBF, was determined by means of ninhydrin assays, as described by Yuan et al. [40]. Samples of the films were cryogenically triturated, dried in a vacuum oven, and a mass of 1.6 mg was then added to a ninhydrin aqueous solution containing $SnCl_2$ and glycol ethylene. The mixture was stirred at 100 °C for 20 min for the reaction of the ninhydrin with the amino groups of chitosan to take place, forming a soluble compound which presents a strong absorption at 570 nm. The concentration of free amine (FA) was determined by optical absorbance, at 570 nm, on a spectrophotometer (model Nova 1800 UV). The percentage of free amine (FA) was calculated as the absorbance of the solution after the

ninhydrin reaction with the crosslinked film (A_C), and the absorbance of the solution after the ninhydrin reaction with the neat chitosan film (A_N):

$$FA = \left(\frac{A_C}{A_N}\right)x100$$

Three measurements were performed for each sample.

2.2.5 Scanning electron microscopy (SEM)

The morphology of the surface of the coated AZ31 sheets and of the free-standing films cross-section were investigated by scanning electron microscopy, using a Jeol microscope (model JSM-639OLV) with an accelerating voltage of 8kV. For the acquisition of the cross-section images, the films were cryogenically broken in liquid nitrogen. All samples were gold sputtered prior to analysis.

3. Results and Discussion

3.1 Coating characterization

As shown in details in a previous publication, chitosan reacts with genipin forming an amide and a cyclic amine group (Figure 1) [12]. This reaction results in a change in the coating color, from pale yellow to deep blue, as well as in changes in the ratio of the amide (1643 cm^{-1}) and amine (1546 cm^{-1}) band heights, in the FTIR spectra, and in the area of the nitrogen 1s binding energy of amines (399.5 eV) and of protonated amine (400.8 eV), in the XPS spectra [12]. All coatings show good adhesion to the substrate.

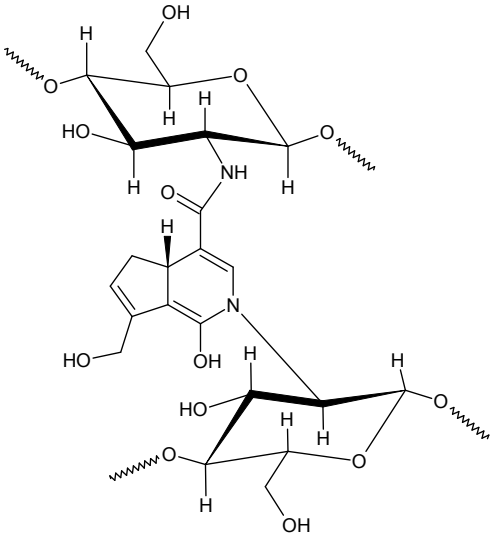

Figure 1: Schematic representation of the chemical structure of chitosan crosslinked with genipin.

In Table 1 it is shown the results of the ninhydrin assay for the prepared films. It can be observed that the percentage of free amine decreases as the amount of added genipin increases, as expected. The crosslinking degree, calculated as $CD = 100\% - FA$, varied from 42 to 64%.

Table 1. Degree of free amine and of crosslinking according to the ninhydrin assay.

Sample	FA (%)	Crosslinking degree (%)
QTG1	58 ± 4	42 ± 4
QTG3	48 ± 2	52 ± 2
QTG6	36 ± 3	64 ± 3

3.2Polarization and EIS

The results of the potentiodynamic polarization are shown in Figure 2. It can be observed that the curves obtained for the coated samples are shifted to lower currents and less negative potentials, in relation to AZ31Gr, indicating a decrease in the thermodynamic tendency for corrosion and in the kinetics of the process. In terms of the shape of the curves, the most significant difference can be observed in the anodic branches. AZ31Gr shows metal dissolution at the corrosion potential, whereas the coated samples present anodic branches with higher slopes. This result suggests that the presence of the coatings inhibits the anodic process, but has insignificant influence on the cathodic one.

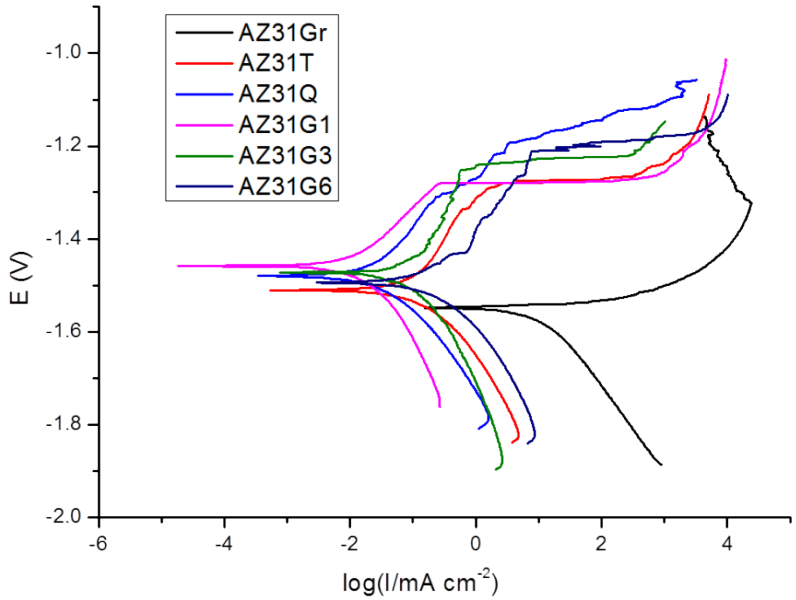

Figure 2: Potentiodynamic polarization curves for the samples after 30 min of exposure to SBF.

Figure 3 shows the impedance spectra for the samples after 1 and 31 days of exposure to the SBF. The spectra were fitted using the circuit models shown in Figures 4a and 4b. The results obtained for the resistance of the chitosan coating ($R_{coating}$), the magnesium hydroxide layer (R_{MgL}), the charge transfer process (R_{ct}) and the capacitance of the chitosan coating ($CPE_{coating}$) are shown in Figures 4c to 4f. It can be observed in Figure 2a that the samples AZ31G1 and AZ31Q present the highest impedance over the entire frequency range, reaching values of the order of $10^5 \Omega\, cm^2$ at low frequencies. After 31 days of exposure, these samples still present impedances in this order of magnitude, at low frequencies, providing the best corrosion protection amongst the samples tested. This impedance value is higher than those reported in the literature for chitosan coatings on pure magnesium and some of its alloys, in SBF medium [19, 25, 44].

These results can be better understood by analyzing how R_{MgL}, $R_{coating}$ and R_{ct} change over time (Figures 4c to 4f). The R_{MgL} values show an increasing tendency for all samples, which suggests the deposition of corrosion products on flaws of the $Mg(OH)_2$ layer. The samples AZ31Q and AZ31G1 present the highest R_{MgL} values after 31 days of exposure (of the order of $10^4 \Omega\, cm^2$), followed by AZ31T. This result can be attributed to a higher efficiency of the neat chitosan coating and of the coating crosslinked with 1 mmol of genipin in controlling the arrival of electrolytes to the $Mg(OH)_2$ layer, which allows for the homogenous build-up of a layer of corrosion products underneath the polymer coating. The lower R_{MgL} values observed for AZ31G3 and AZ31G6 from the beginning of the measurements suggests that the $Mg(OH)_2$ layer underneath these coatings is damaged, probably due to reactions with the acetic acid present in the chitosan solutions used for the coating process (in fact, the initial R_{MgL} values observed for AZ31Q, AZ31G1, AZ31G3 and AZ31G6 are lower than that for AZ31T, corroborating this assumption). This also indicates that the coatings crosslinked with 3 mmol and 6 mmol of genipin are less efficient in controlling the diffusion of the electrolyte.

The samples AZ31Q and AZ31G1 also present the highest $R_{coating}$ values (of the order of $10^5 \Omega\, cm^2$) corroborating the conclusion that the neat chitosan coating and the chitosan coating crosslinked with 1 mmol of genipin have the best barrier properties.

The $R_{coating}$ values increase during the measurement, which is related to the occurrence of further crosslinking in the coating, due to the presence of bivalent cations in the SBF solution (described in detail in the next section). In fact, the literature reports that chitosan can be crosslinked by bivalent cations such as Mg^{2+} and Ca^{2+}, present in the SBF [33]. The samples AZ31G3 and AZ31G6 show the lowest $R_{coating}$ values, indicating low barrier properties for these coatings. On comparing the values for R_{MgL}, $R_{coating}$ and R_{ct} shown in Figures 4c to 4e, it can be concluded that the high impedance observed in Figure 3 for AZ31Q and AZ31G1, is mainly related to the barrier properties of their chitosan coating.

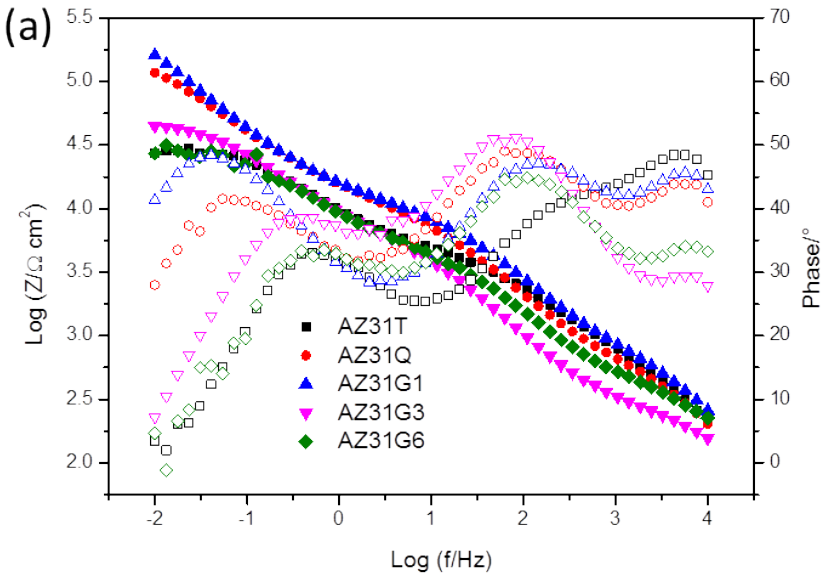

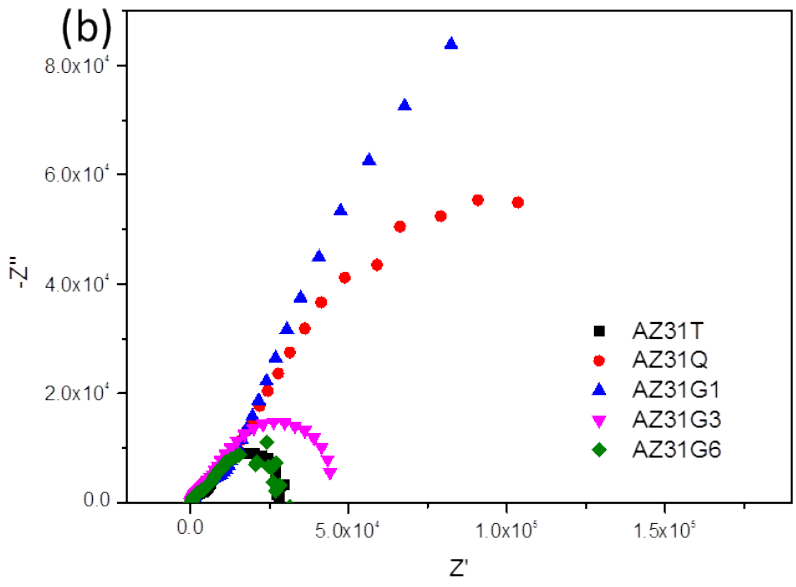

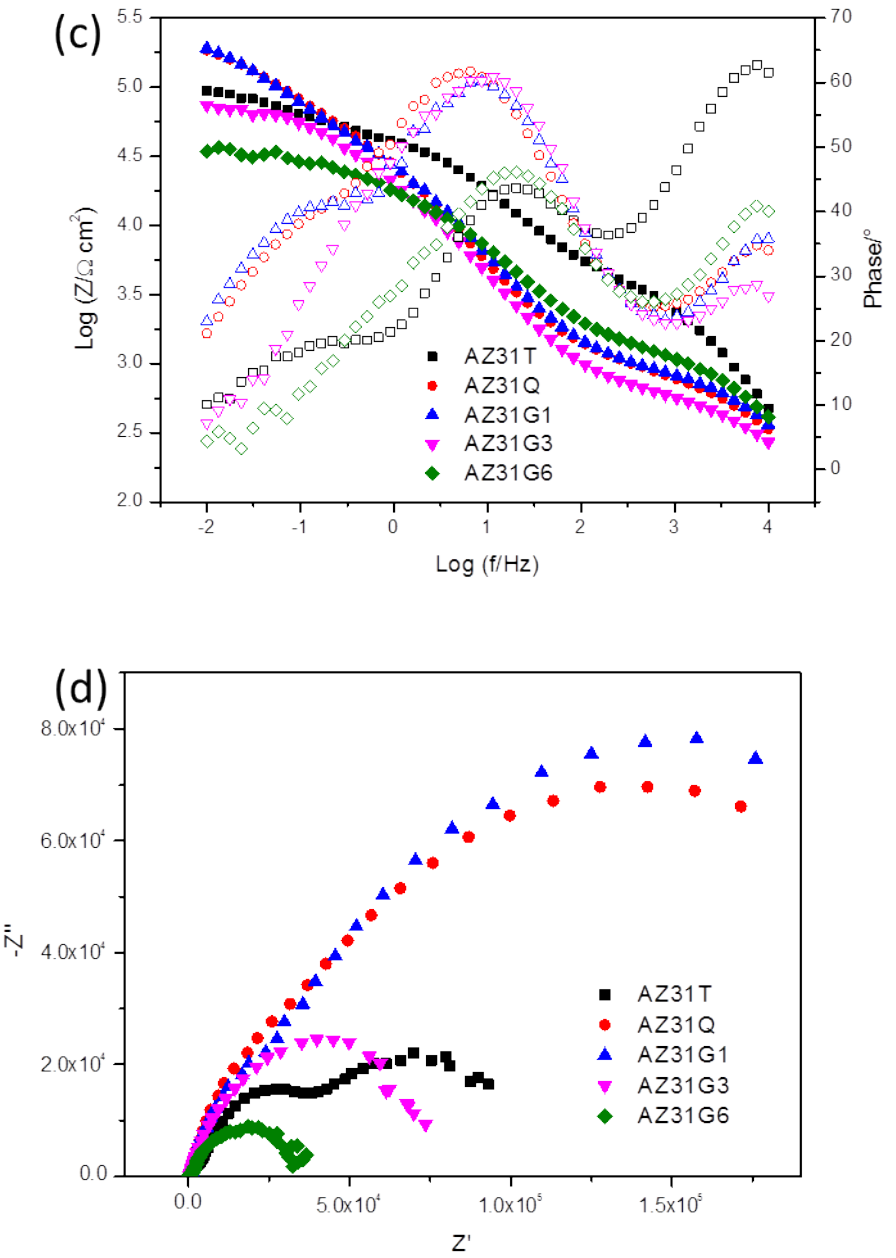

Figure 3: Impedance spectra obtained for the samples after 1 and after 31 days of exposure to the SBF medium: (a) Bode and phase - day 1; (b) Nyquist plot - day 1; (c) Bode and phase - day 31; (d) Nyquist plot – day 31.

Additionally, Figure 3a shows the presence of three time constants in the phase angle (described in the circuit models with constant phase elements, CPEs), which are attributed to the chitosan coating ($CPE_{coating}$), the magnesium hydroxide layer (CPE_{MgL}) and the electric double layer (CPE_{DL}). Figure 4f shows that, for all samples, the values of $CPE_{coating}$ do not increase regularly over time, but an increase is observed after 31 days in comparison to the initial value. The impedance of the protective polymer

coatings is expected to increase during their exposure to a corrosive solution as a consequence of the uptake of electrolytes, which have a much greater dielectric constant than the polymeric film. As shown in Figure 4f, the samples AZ31G1 and AZ31Q present the highest $CPE_{coating}$ values, a result that is related to the higher ionic absorption of their coatings, due to the occurrence of crosslinking.

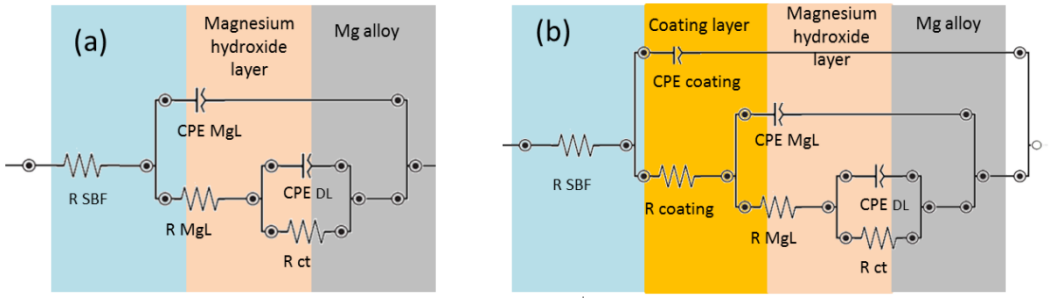

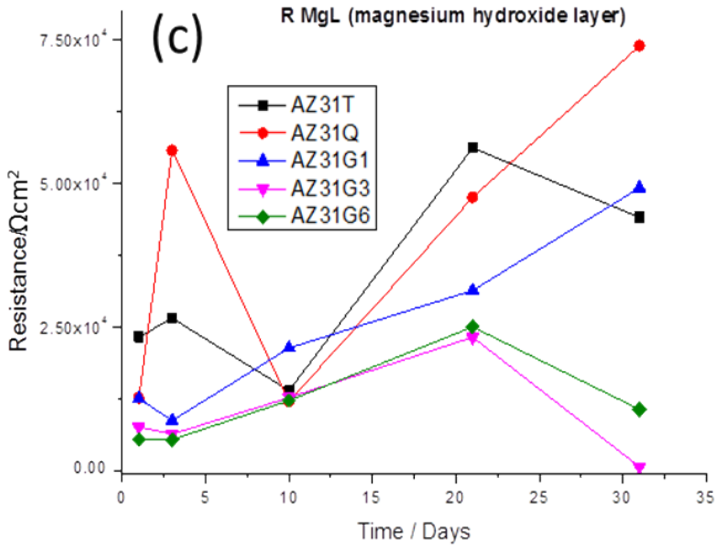

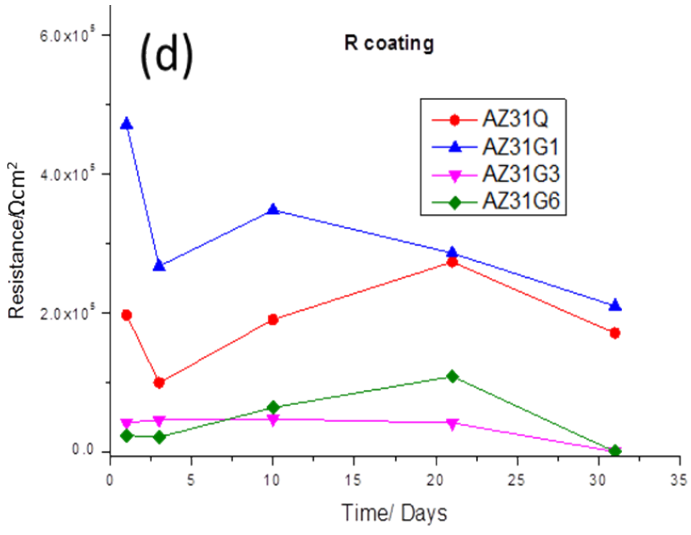

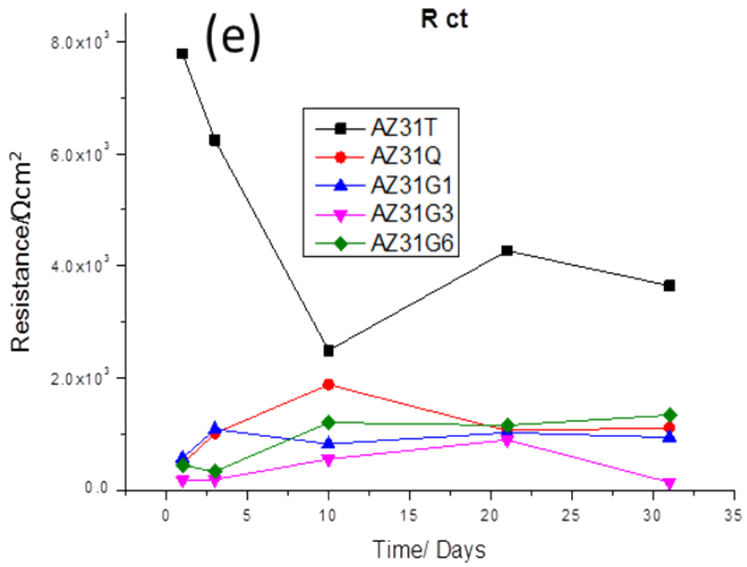

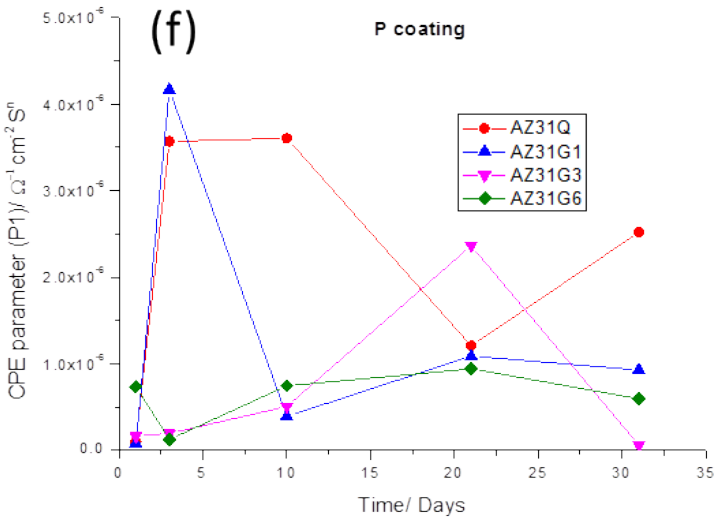

Figure 4: (a) Equivalent circuit used to fit EIS data for AZ31 T. (b) Equivalent circuit used to fit EIS data for bi-layered Mg alloys. Evolution of (c) R_{MgL}, (d) $R_{coating}$, (e) R_{ct} and (f) $CPE_{coating}$ over time.

3.3 Hydrogen evolution

Figure 5 shows the cumulative hydrogen gas evolution for AZ31Gr, AZ31T and AZ31G1. It can be observed that the coating considerably decreases the hydrogen evolution rate during the whole period of test. A controlled release of hydrogen is very important for magnesium implants to avoid the formation of subcutaneous cavities related to hydrogen gas accumulation [36, 37]. In the study of Song et al. [45] it is suggested that a hydrogen evolution rate of 0.01 mL cm^{-2} day^{-1} is acceptable for magnesium implants, and different studies have used this value as a reference since then. As can be seen in Figure 5a, the overall hydrogen evolution rate for AZ31G1

complies with this acceptable level (the average rate, after 7 days, is of 0.06 mL cm^{-2} day^{-1}, which implies an overall rate below 0.01 mL cm^{-2} day^{-1}), despite some periods of slightly higher rates.

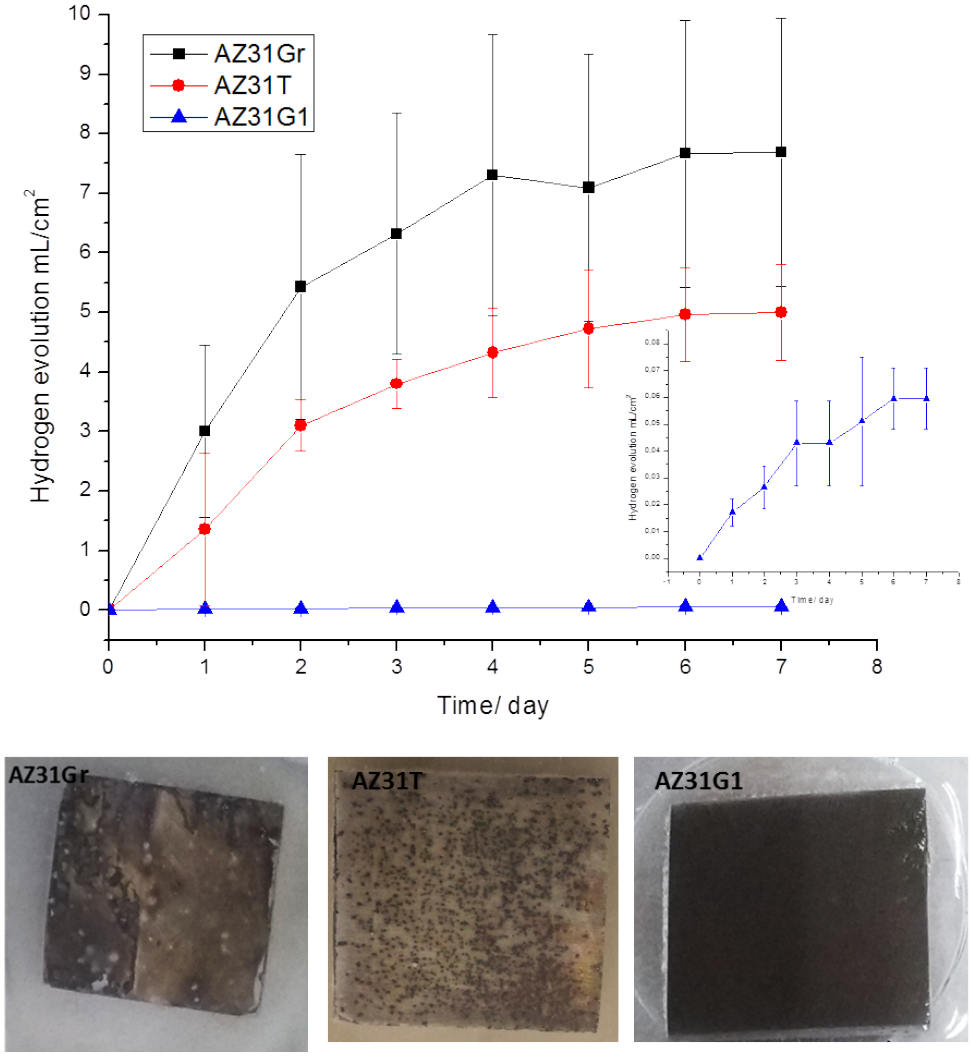

Figure 4: (a) Hydrogen evolution rate for AZ31Gr, AZ31T and AZ31G1. (b) Aspect of AZ31Gr, AZ31T and AZ31G1 samples after seven days of exposure to the SBF.

Additionally, Figure 4b shows the aspect of AZ31Gr, AZ31T and AZ31G1 after 7 days of exposure to the corrosive solution. It can be observed that AZ31Gr and AZ31T shows uniform and pit corrosion while AZ31G1 shows no signs of corrosive attack. Furthermore, the lack of blisters in the coating of AZ31G1 indicates a good adhesion between the chitosan coating and the NaOH treated substrate.

3.4 Crosslinking and morphology

In a previous publication it was reported that the level of protection provided by chitosan coatings increases with the degree of crosslinking, in corrosion tests performed with 3.5 wt.% NaCl solution [12]. As mentioned above, this relation was not observed in the study reported herein, which could be due to the occurrence of interactions between the SBF and the chitosan coatings that resulted in an increase in the degree of crosslinking. To test this hypothesis, the ninhydrin test was applied to free-standing chitosan films prepared in the same way as the coatings, before and after immersion in SBF. The results are shown in Table 2.

It can be observed that, after the immersion in SBF the overall percentage of free amine is considerably reduced. Furthermore, the percentage of free amine does not follow a regular trend according to the initial crosslinking degree. This change in the percentage of free amine confirms that the exposure to SBF increases the crosslinking degree of the chitosan films. This conclusion is further corroborated by the fact that, after the immersion of the films in the 3.5 wt.% NaCl aqueous solution, a much lower decrease in the percentage of free amine is observed (for QTG1 and QTG6 the differences are within the standard deviation) and the initial order is preserved.

Thus, considering the results obtained with the electrochemical characterizations, it can be concluded that, under the conditions reported herein, chitosan coatings must be either neat (not crosslinked) or have an initial crosslinking degree of up to 42% (which corresponds to an initial degree of free amine of 58%) to provide good anticorrosive properties for magnesium alloys in SBF. A possible explanation for this result is that a crosslinking degree of up to 42% results in chitosan coatings with higher $R_{coating}$ values and, consequently, with better anticorrosive properties. However, at higher crosslinking degrees the coatings may become brittle and susceptible to the formation of cracks [46, 47].

To investigate whether the inferior performance of the sample AZ31G6 could be related to the presence of cracks on the coatings, the morphology of this sample surface was investigated by means of SEM. Figure 5 shows micrographs of the surfaces of the samples AZ31Q and AZ31G6 after the corrosion tests. It can be observed that the area of AZ31G6 which was exposed to the corrosive solution presents cracks, whereas no cracks are observed on the exposed area of AZ31Q. This result corroborates the

conclusion that the inferior level of protection offered by the coating crosslinked with 6 mmol of genipin is related to the coating fragility.

Table 2. Degree of free amine in the films before and after immersion in SBF and in a 3.5% NaCl solution.

Sample	FA before swelling (%)	FA after swelling in SBF (%)	FA after swelling in 3.5wt.% NaCl (%)
QTG1	58 ± 4	27 ± 3	50 ± 2
QTG3	48 ± 2	32 ± 2	40 ± 1
QTG6	36 ± 3	25 ± 2	32 ± 2

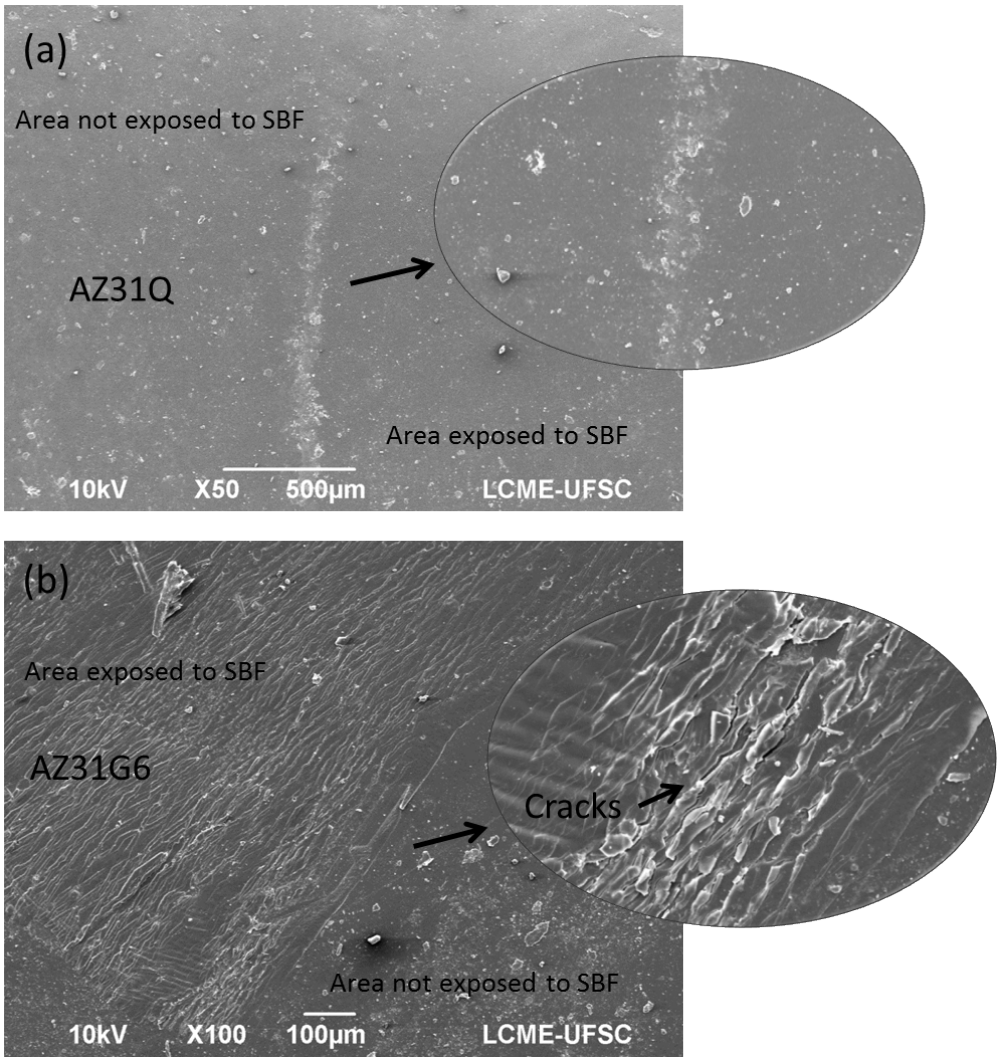

Figure 5: Micrographs of the surface of samples AZ31Q (a) and AZ31G6 (b) after exposure to the SBF under the same conditions applied in the corrosion tests. The insets show the exposed surfaces at higher magnification.

Additionally, the morphology of the cross-section of free-standing films, before and after immersion in SBF, was investigated by SEM. In a previous publication by the authors [12], it was reported that the morphology of neat chitosan films was considerably modified after immersion in a corrosive solution. This change in morphology was correlated to the water uptake, the parameter considered to be responsible for the differences in the performance of the coatings in 3.5 wt.% NaCl solution. The intensity of this morphological change decreased with the crosslinking degree, and no change was observed for the film crosslinked with 6 mmol of genipin. As shown in Figure 6, the morphology of the films prepared in this study does not change after immersion in SBF. This result is related to the increase in the degree of crosslinking that takes place during immersion, as previously mentioned, which decreases the water uptake.

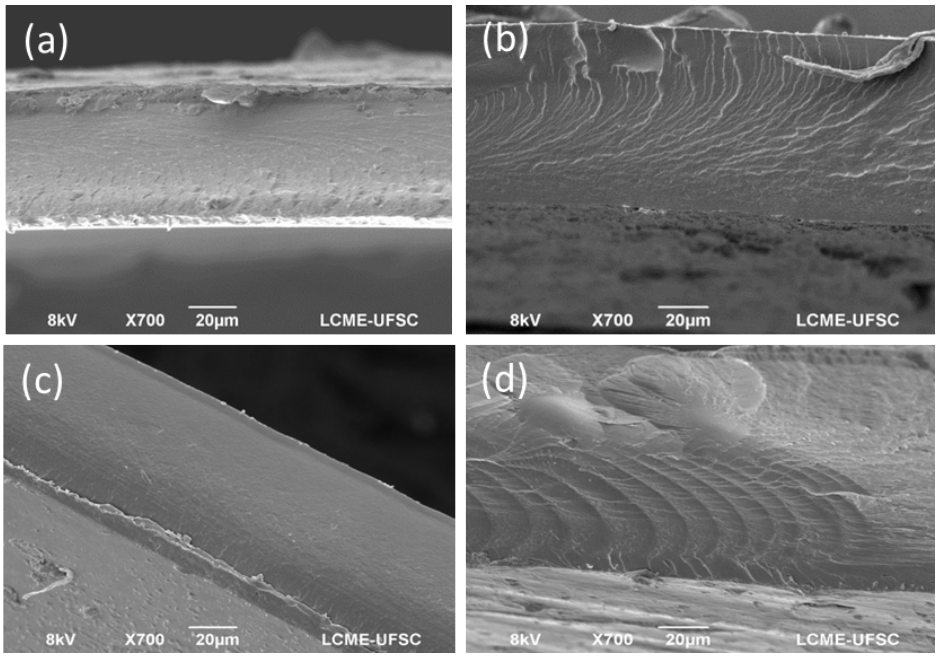

Figure 6: Morphology of the fracture of QT films before (a) and after (b) immersion in SBF and of QTG6 films before (c) and after (d) immersion in SBF.

4. Conclusions

Coatings of neat chitosan and of chitosan crosslinked with 1 mmol of genipin are efficient in protecting the magnesium alloy AZ31 from corrosion in SBF. The corrosion protection provided by these coatings, in polarization and ESI tests, is superior to that observed for similar coatings described in the literature. In contrast to the results obtained using a 3.5 wt.% NaCl solution, an increase in the crosslinking degree is not beneficial to the level of protection of the coatings in SBF. This result is related to the fact that the coating interacts with cations present in the SBF, and its degree of crosslinking increases until values at which the film becomes fragile and susceptible to cracking, as confirmed by the SEM analysis. Nevertheless, the hydrogen evolution rate observed for the sample coated with chitosan crosslinked with 1mmol of genipin, complies with the tolerance limit, a result that indicates the potential of this coating in protection magnesium alloy implants.

5. Acknowledgments

This work was supported by the Conselho Nacional de Pesquisa, CNPq [grant 445263/2014-8].

Data Availability

The raw/processed data required to reproduce these findings cannot be shared at this time due to technical or time limitations.

References

[1] NACE, International measures of prevention, application, and economics of corrosion technologies study. (2016).

[2] C.H. Ye, Y.F. Zheng, S.Q. Wang, T.F. Xi, Y.D. Li, In vitro corrosion and compatibility study of phytic acid modified WE43 magnesium alloy, Appl. Surf. Sci. 258, (2012) 3420-3427. https://doi.org/10.1016/j.apsusc.2011.11.087

[3] Z. Zhen, T.F. Xi, Y.F. Zheng, Surface modification by natural biopolymer coatings on magnesium alloys for biomedical applications, in: T.S.N. Narayanan, I.S. Park, M.H. Lee, Surface Modification of magnesium and its alloys for biomedical applications: Vol 2, Woodhead-Publishing, Cambridge, 2015, pp.301-333.

[4] G.P. Abatti, A.T.N. Pires, A. Spinelli, N. Scharnagl, T.F. da Conceição, Conversion coating on magnesium alloy sheet (AZ31) by vanillic acid treatment: Preparation, characterization and corrosion behavior, J. Alloys Compd. 738, 2018, 224–232. https://doi.org/10.1016/j.jallcom.2017.12.115

[5] W.F. Ng, M.H. Wong, F.T. Cheng, Stearic acid coating on magnesium for enhancing corrosion resistance in Hank's solution, Surf. Coat. Technol. 204, 2010, 1823-1830. https://doi.org/10.1016/j.surfcoat.2009.11.024

[6] K. Azzaoui, E. Mejdoubi, S. Jodeh, A. Lamhamdi, E. Rodriguez-Castelión, M. Algarr, A. Zarrouk, A. Errich, R. Salghi, H. Lgaz, Eco friendly green inhibitor Gum Arabic (GA) for the corrosion control of mild steel in hydrochloric acid medium, Corros. Sci. 129, 2017, 70–81. https://doi.org/10.1016/j.corsci.2017.09.027

[7] K. Zhang, W. Yang, X. Yin, Y. Chen, Y. Liu, J. Le, B. Xu, Amino acids modified konjac glucomannan as green corrosion inhibitors for mild steel in HCl solution, Carbohydr. Polym. 181, 2018, 191–199. https://doi.org/10.1016/j.carbpol.2017.10.069

[8] Y. Sangeetha, S. Meenakshi, C.S. Sundaram, Investigation of corrosion inhibitory effect of hydroxyl propyl alginate on mild steel in acidic media, J. Appl. Polym. Sci. 133(7), 2016 6–11. https://doi.org/10.1002/app.43004

[9] M.M. Fares, A.K. Maayta, M.M. Al-Qudah, Pectin as promising green corrosion inhibitor of aluminum in hydrochloric acid solution, Corros. Sci. 60, 2012, 112–117. https://doi.org/10.1016/j.corsci.2012.04.002

[10] S.A. Umoren, U.M. Eduok, Application of carbohydrate polymers as corrosion inhibitors for metal substrates in different media: A review, Carbohydr. Polym. 140, 2016, 314–341. https://doi.org/10.1016/j.carbpol.2015.12.038

[11] J. Carneiro, J. Tedim, M.G.S. Ferreira, Chitosan as a smart coating for corrosion protection of aluminum alloy 2024: A review, Prog. Org. Coat. 89, 2015, 348–356. https://doi.org/10.1016/j.porgcoat.2015.03.008

[12] L.Y. Pozzo, T.F. da Conceição, A. Spinelli, N. Scharnagl, A.T.N. Pires, Chitosan coatings crosslinked with genipin for corrosion protection of AZ31 magnesium alloy sheets, Carbohydr. Polym. 181, 2018, 71–77. https://doi.org/10.1016/j.carbpol.2017.10.055

[13] Z. Zhong, J. Qin, J. Ma, Cellulose acetate/hydroxyapatite/chitosan coatings for improved corrosion resistance and bioactivity, Mater. Sci. Eng. C 49, 2015, 251–255. https://doi.org/10.1016/j.msec.2015.01.020

[14] M. Farrokhi-Rad, T. Shahrabi, S. Mahmoodi, S. Khanmohammadi, Electrophoretic deposition of hydroxyapatite-chitosan-CNTs nanocomposite coatings, Ceram. Int. 43(5), 2017, 4663–4669. https://doi.org/10.1016/j.ceramint.2016.12.139

[15] M.M. Solomon, H. Gerengi, T. Kaya, S.A. Umoren, Performance evaluation of a chitosan/silver nanoparticles composite on St37 corrosion in a 15% HCl solution, ACS Sustain. Chem. Eng. 5, 2017, 809-820.

[16] D. Jugowiec, A. Łukaszczyk, Ł. Cieniek, K. Kowalski, Ł. Rumian, K. Pietryga, T. Moskalewicz, Influence of the electrophoretic deposition route on the microstructure and properties of nano-hydroxyapatite/chitosan coatings on the Ti-13Nb-13Zr alloy, Surf. Coat. Technol. 324, 2017, 64–79. https://doi.org/10.1016/j.surfcoat.2017.05.056

[17] L.L. de Sousa, V.P. Ricci, D.G. Prado, R.C. Apolinário, L.C.O. Vercik, E.C.S. Rigo, M.C.S. Fernandes, N.A. Mariano, Titanium Coating with Hydroxyapatite and Chitosan Doped with Silver Nitrate, Mater. Res. 20, 2017, 863-868.

[18] H. Hassannejad, M. Moghaddasi, E. Saebnoori, A.R. Baboukani, Microstructure, deposition mechanism and corrosion behavior of nanostructured cerium oxide conversion coating modified with chitosan on AA2024 aluminum alloy, J. Alloys Compd. 725, 2017, 968–975. https://doi.org/10.1016/j.jallcom.2017.07.253

[19] A.M. Fekry, A.A. Ghoneim, M.A. Ameer, Electrochemical impedance spectroscopy of chitosan coated magnesium alloys in a synthetic sweat medium, Surf. Coat. Technol. 238, 2014, 126–132. https://doi.org/10.1016/j.surfcoat.2013.10.058

[20] S. Heise, M. Höhlinger, Y.T. Hernández, J.J.P. Palacio, J.A.R. Ortiz, V. Wagener, A.R. Boccaccini, Electrophoretic deposition and characterization of chitosan/bioactive glass composite coatings on Mg alloy substrates, Electrochim. Acta, 232, 2017, 456–464. https://doi.org/10.1016/j.electacta.2017.02.081

[21] K. Bai, Y. Zhang, Z. Fu, C. Zhang, X. Cui, E. Meng, S. Guan, J. Hu, Fabrication of chitosan/magnesium phosphate composite coating and the in vitro degradation properties of coated magnesium alloy, Mater. Lett. 73, 2012, 59–61. https://doi.org/10.1016/j.matlet.2011.12.102

[22] J. Carneiro, J. Tedim, S.C.M. Fernandes, C.S.R Freire, A. Gandini, M.G.S. Ferreira, M.L. Zheludkevich, Functionalized chitosan-based coatings for active corrosion protection, Surf. Coat. Technol. 226, 2013, 51–59. https://doi.org/10.1016/j.surfcoat.2013.03.035

[23] L.C. Córdoba, A. Marques, M. Taryba, T. Coradin, M.F. Montemor, Hybrid coatings with collagen and chitosan for improved bioactivity of Mg alloys, Surf. Coat. Technol. 341, 2018, 103-113. https://doi.org/10.1016/j.surfcoat.2017.08.062

[24] H. Gao, M. Zhang, J. Zhao, L. Gao, M. Li, In vitro and in vivo degradation and mechanical properties of ZEK100 magnesium alloy coated with alginate, chitosan and mechano-growth factor, Mater. Sci. Eng. C, 63, 2016, 450–461. https://doi.org/10.1016/j.msec.2016.02.073

[25] P. L. Jiang, R.Q. Hou, C.D. Chen, L. Sun, S.G. Dong, J.S. Pan, C.J. Lin, Controllable degradation of medical magnesium by electrodeposited composite films of mussel adhesive protein (Mefp-1) and chitosan, J. Colloid Interf. Sci. 478, 2016, 246–255. https://doi.org/10.1016/j.jcis.2016.06.001

[26] T. Sugama, M. Cook, Poly(itaconic acid)-modified chitosan coatings for mitigating corrosion of aluminum substrates, Prog. Org. Coat., 38, 2000, 79-87.

[27] M. Esmaily, J.E. Svensson, S. Fajardo, N. Birbilis, G.S. Frankel, S. Virtanen, R. Arrabal, S. Thomas, L.G. Johansson, Fundamentals and advances in magnesium alloy corrosion, Prog. Mater. Sci. 89, 2017, 92-193.

[28] C. Blawert, D. Fechner, D. Höcher, V. Heitman, W. Dietzel, K.U. Kainer, P. Zivanovic, C. Scharf, A. Ditze, J. Gröbner, S. Schmid-Fetzer, Magnesium secondary alloys: Alloy design for magnesium with improved tolerance limits against impurities, Corros. Sci. 52, 2010, 2452-2468.

[29] N. Hort, Y. Huang, D. Fechner, M. Störmer, C. Blawert, F. Wite, C. Vogt, H. Drücker, R. Willumeit, K.U. Kainer, F. Feyerabend, Magnesium alloys as implant materials – Principles of property design for Mg-RE alloys. Acta Biomater. 6, 2010, 1714-1725.

[30] J. E. Gray, B. Luan, Protective coatings on magnesium and its alloys - a critical review, J. Alloys Compd. 1-2, 2002, 88-113.

[31] T.F. da Conceição, N. Scharnagl, W. Dietzel, K.U. Kainer, Controlled degradation of a magnesium alloy in simulated body fluid using hydrofluoric acid treatment followed by polyacrylonitrile coating, Corros. Sci. 62, 2012, 83-89.

[32] T.F. da Conceição, N. Scharnagl, W. Dietzel, C. Blawert, K.U. Kainer,. Corrosion protection of magnesium alloy AZ31 sheets by spin coating process with poly(ether imide) [PEI], Corros. Sci. 52, 2010, 2066-2079.

[33] S. Heise, S. Virtanen, A.R. Boccaccini, Tackling Mg alloy corrosion by natural polymer coatings - A review, J. Biomed. Mater. Res. A 104A(10), 2016, 2628–2641. https://doi.org/10.1002/jbm.a.35776

[34] N. Scharnagl, C. Blawert, Polymer-based degradable coatings for metallic biomaterials, in: C.Wen (Ed), Surface Coating and Modification of Metallic Biomaterials, Woodhead Publishing, 2015, pp.393-422. http://dx.doi.org/10.1016/B978-1-78242-303-4.00014-4

[35] W.A. Zoubi, Y.G. Ko, Flowerlike organic-inorganic coating responsible for extraordinary corrosion resistance via self-assembly of an organic compound, ACS Sustain. Chem. Eng., 6, 2018, 3546-3555.

[36] F. Witte, Reprint of: The history of biodegradable magnesium implants: A review, Acta Biomater. 6, 2010, 1680–1692. https://doi.org/10.1016/j.actbio.2015.07.017

[37] D. Zhao, F. Witte, F. Lu, J. Wang, J. Li, L. Qin, Current status on clinical applications of magnesium-based orthopaedic implants: A review from clinical translational perspective, Biomaterials, 112, 2017, 287–302. https://doi.org/10.1016/j.biomaterials.2016.10.017

[38] I. Adekanmbi, C.Z. Mosher, H.H. Lu, M. Riehle, H. Kubba, K.E. Tanner, Mechanical behaviour of biodegradable AZ31 magnesium alloy after long term in vitro degradation, Mater. Sci. Eng., C 77, 2017, 1135-1144. . http://dx.doi.org/10.1016/j.msec.2017.03.216

[39] Z. Chun-Yan, Z. Rong-Chang, L. Cheng-Long, G. Jia-Cheng, Comparison of calcium phosphate coatings on Mg-Al and Mg-Ca alloys and their corrosion behavior in Hank's solution, Surf. Coat. Technol. 204, 2010, 3636-3640.

[40] Y. Yuan, B.M. Chesnutt, G. Utturkar, W.O. Haggard, Y. Yang, J.L. Ong, J.D. Bumgardner, The effect of crosslinking of chitosan microspheres with genipin on protein release, Carbohydr. Polym. 68, 2007, 561–567.

[41] C. Liu, Y. Xin, X. Tian, P.K. Chu, Corrosion behavior of AZ91 magnesium alloy treated by plasma immersion ion implantation and deposition in artificial physiological fluids, Thin Solid Films 516, 2007, 422-427. https://doi.org/10.1016/j.tsf.2007.05.048

[42] X.N. Gu, Y.F. Zheng, Q.X. Lan, Y. Cheng, Z.X. Zhang, T.F. Xi, D.Y. Zhang, Surface modification of an Mg-1Ca alloy to slow down its biocorrosion by chitosan, Biomed. Mater. 4(4), 2009, 1–5. https://doi.org/10.1088/1748-6041/4/4/044109

[43] A. Yamamoto, S. Hiromoto, Effect of inorganic salts, amino acids and proteins on the degradation of pure magnesium in vitro, Mater. Sci. Eng., C 29, 2009, 1559-1568. https://doi.org/10.1016/j.msec.2008.12.015

[44] H.R. Tiyyagura, R. Rudolf, S. Gorgieva, R. Fuchs-Godec, B.V. Rao, M.K. Mohan, V. Kokol, The chitosan coating and processing effect on the physiological corrosion behavior of porous magnesium monoliths, Prog. Org. Coat. 99, 2016, 147-156.

[45] G. Song, Control of biodegradation of biocompatible magnesium alloys, Corros. Sci, 49, 2007, 1696-1701.

[46] R.A.A. Muzzarelli, Genipin-crosslinked chitosan hydrogels as biomedical and pharmaceutical aids, Carbohydr. Polym. 77, 2009, 1–9. https://doi.org/10.1016/j.carbpol.2009.01.016

[47] V. Chiono, E. Pulieri, G. Vozzi, G. Ciardelli, A. Ahluwalia, P. Giusti, Genipin-crosslinked chitosan/gelatin blends for biomedical applications, J. Mater. Sci.: Mater. Med. 19, 2008, 889-898. https://doi.org/10.1007/s10856-007-3212-5